ACS APPLIED MATERIALS & INTERFACES

Research Article

www.acsami.org

NiO/SiC Nanocomposite Prepared by Atomic Layer Deposition Used as a Novel Electrocatalyst for Nonenzymatic Glucose Sensing

Peng Yang,[†,‡] Xili Tong,[†] Guizhen Wang,[§] Zhe Gao,[†] Xiangyun Guo,[†] and Yong Qin*[,†]

[†]State Key Laboratory of Coal Conversion, Institute of Coal Chemistry, Chinese Academy of Science, Taiyuan 030001, China

[‡]University of Chinese Academy of Sciences, Beijing 100049, China

[§]Key Laboratory of Chinese Education Ministry for Tropical Biological Resources, Hainan University, Haikou 570228, China

ABSTRACT: NiO nanoparticles are deposited onto SiC particles by atomic layer deposition (ALD). The structure of the NiO/SiC hybrid material is investigated by inductively coupled plasma atomic emission spectrometry (ICP-AES), X-ray photoelectron spectroscopy (XPS), and transmission electron microscopy (TEM). The size of the NiO nanoparticles is flexible and can be adjusted by altering the cycle number of the NiO ALD. Electrochemical measurements illustrate that NiO/SiC prepared with 600 cycles for NiO ALD exhibits the highest glucose sensing ability in alkaline electrolytes with a low detection limit of 0.32 μM (S/N = 3), high sensitivity of 2.037 mA mM^{-1} cm^{-2}, a linear detection range from approximately 4 μM to 7.5 mM, and good stability. Its sensitivity is about 6 times of that for commercial NiO nanoparticles and NiO/SiC nanocomposites prepared by a traditional incipient wetness impregnation method. It is revealed that the superior electrochemical ability of ALD NiO/SiC is ascribed to the strong interaction between NiO and the SiC substrate and the high dispersity of NiO nanoparticles on the SiC surface. These results suggest that ALD is an effective way to deposit NiO on SiC for nonenzymatic glucose sensing.

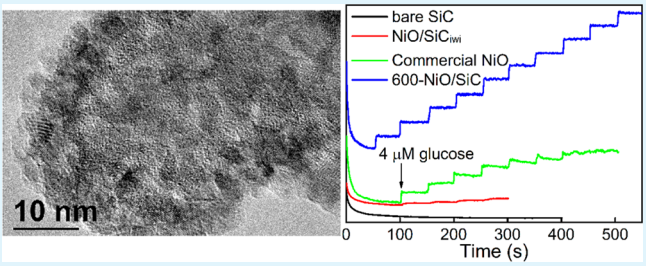

KEYWORDS: *NiO nanoparticles, atomic layer deposition, silicon carbide, glucose sensor, nonenzymatic, electrocatalysis*

INTRODUCTION

Quantitative detection of glucose is of great importance due to its promising application in many fields, such as food processing, clinical diagnosis, environmental monitoring, and in developing renewable fuel cells.[1−4] Many approaches have been developed for glucose sensing.[5,6] In general, the electrochemical technique holds great promise for the construction of glucose biosensors based on its simplicity, high sensitivity, good selectivity, and low cost.[7] Since Clark and Lyons developed the first enzymatic glucose biosensor in 1962,[8] extensive attention has been paid to developing electrochemical glucose biosensors. These glucose sensors usually involved the use of enzymes such as glucose oxidase at the early stages.[9] Enzyme-based glucose sensors exhibit high sensitivity and selectivity for glucose. However, such biosensors require complicated immobilization procedures and exhibit poor long-term stability. Moreover, their sensing abilities are easily affected by pH and temperature during measurements due to the nature of enzyme.[10] As a result, increasing attempts have been undertaken to develop nonenzymatic glucose biosensors based on noble metals (such as Pt, Au, Pd), alloys (Pt−Pb, Pt−Ru, Pt−Au, etc.), oxides (such as NiO, CuO, Cu_2O, Co_3O_4, MnO_2, ZnO), and their composites with CNT or graphene.[11−14] Among these, NiO has been widely utilized and is proven to be an effective electrocatalyst for glucose sensing because of its strong electrocatalytic activity, low cost, and high organic capturing ability.[15,16] The mechanism of glucose oxidation by NiO-based materials is explained by the following reactions. First, NiOOH is formed by the interaction of NiO with OH^- in alkaline solution. Glucose is then oxidized to glucolactone by NiOOH, which is deoxidized to NiO at the same time.[17] As is well known, the electrocatalytic activity of nanoparticles is significantly dependent on their size and distribution.[18,19] To date, various techniques, such as electrochemical deposition and hydrothermal synthesis, have been employed to prepare NiO-based nanostructures as glucose sensors.[20−22] However, these traditional methods have no good control over the size or distribution of NiO. In addition, it is reported that NiO-based glucose sensors have difficulty in maintaining long-term stability because of the gradual detachment and dissolution of the catalyst from the substrate.[23,24]

In the present work, NiO/SiC nanocomposites were prepared by the atomic layer deposition (ALD) technique and employed as nonenzymatic glucose sensing electrocatalysts. ALD is a promising approach for catalyst synthesis due to its outstanding advantages.[25] It has been applied in many areas because of its precise control over particle size and distribution.[26,27] SiC is an excellent catalyst support with stable physical and chemical properties, high thermal conductivity, and no toxicity.[28−30] It is attracting more and more attention in

Received: December 3, 2014
Accepted: February 9, 2015
Published: February 9, 2015

DOI: 10.1021/am508508m
ACS Appl. Mater. Interfaces 2015, 7, 4772−4777

electrochemical and bioelectrochemical applications due to its biocompatibility, wider potential window, and lower background current.[31,32] Herein, we took advantage of these desirable features of the ALD technique and SiC substrate and synthesized NiO/SiC nanocomposites, which present remarkable performance in nonenzymatic glucose sensing. To the best of our knowledge, this is the first time that NiO/SiC nanocomposites prepared by ALD have been applied to glucose detection.

EXPERIMENTAL SECTION

Preparation of NiO/SiC. SiC particles with a high specific surface area of 50.8 m^2 g^{-1} were synthesized through a sol−gel and carbothermal reduction method reported previously.[33] SiC particles were dispersed in anhydride ethanol under proper agitation in an ultrasonic bath, dropped onto a quartz wafer, and air-dried. Then, ALD of NiO was carried out in a homemade, hot-wall, closed chamber-type ALD reactor at 250 °C using nickelocene ($NiCp_2$) and O_3 as precursors. The $NiCp_2$ source was held at 65 °C. After deposition of NiO, the sample was collected and is denoted as X-NiO/SiC, where X means the cycle number of the NiO ALD.

For comparison, NiO and SiC nanocomposites with the same NiO content as that of 600-NiO/SiC was synthesized through an incipient wetness impregnation method (denoted as NiO/SiC_{iwi}). $Ni(NO_3)_2{\cdot}6H_2O$ (530 mg) was added to 50 mL ethanol under magnetic stirring. After the solution became transparent, 900 mg of SiC was carefully added. The suspension was held for 24 h under magnetic stirring to all for sufficient contact of $Ni(NO_3)_2$ with SiC. Then, the suspension was allowed to dry at 40 °C under continuous magnetic stirring. The sample was calcined at 500 °C for 5 h in a muffle oven to obtain NiO/SiC_{iwi}.

Characterization. The Ni content was detected through a Thermo iCAP 6300 inductively coupled plasma atomic emission spectrometer (ICP-AES). X-ray photoelectron spectroscopy (XPS) was employed on a XSAM 800 X-ray photoelectron spectrometer (Kratos, UK). Transmission electron microscopy (TEM) images were obtained on a JEOL-2100F microscope.

Electrochemical Testing. Electrochemical measurements were performed with a CHI 760D electrochemical workstation (CH Instrument, Shanghai, China). A conventional three-electrode system was employed consisting of a glassy carbon electrode (GCE) modified with NiO/SiC samples as the working electrode, a platinum foil electrode as the counter electrode, and a Hg/HgO electrode as the reference electrode. All of the electrochemical experiments were performed in an aqueous 1 M KOH solution. To prepare modified electrodes, we dispersed 5 mg of electroactive material into a 1 mL mixed solution of ethanol and nafion (volume ratio 49:1 $v_{ethanol}/v_{nafion}$) under ultrasonication for 30 min. Then, a 3 μL portion of the resulting suspension was cast on the surface of bare GCE (diameter of 3 mm) and allowed to air dry for about 15 min. The cyclic voltammetry (CV) of the samples was measured over a potential range from 0.2 to 0.6 V at a scan rate of 50 mV s^{-1}. The electrochemical impedance spectroscopy (EIS) measurements were conducted with a frequency ranging from 10^5 to 0.01 Hz at the applied potential of 0.4 V with an AC perturbation of 5 mV. Chronoamperometry was performed at an applied potential of 0.5 V under 300 rpm magnetic stirring with glucose added stepwise. For comparison, glucose sensing measurements were also taken with bare SiC, commercial NiO nanoparticles (50 nm), and NiO/SiC_{iwi} modified electrodes.

RESULTS AND DISCUSSION

Structural Analysis of NiO/SiC. TEM was employed to examine the morphology and microstructure of the NiO/SiC nanocomposites produced. Figure 1 shows TEM and high resolution TEM (HRTEM) images of 200-, 400-, 600-, and 800-NiO/SiC samples. With an increasing number of ALD cycles, the size of the NiO nanoparticles increases and their distribution gets denser. The average sizes of the NiO nanoparticles of 200-, 400-, and 600-NiO/SiC are approximately 2.2, 3.2, and 4.2 nm, respectively. In Figure 1h, the NiO nanoparticles of 800-NiO/SiC form a continuous film due to large particle size and high density. The surface active sites on individual NiO nanoparticle will decrease due to the overlap between the NiO nanoparticles, which may reduce their activity. From the insets in Figure 1f, lattice spacings of 0.24 and 0.21 nm are observed, corresponding to the (111) and (200) crystal planes of NiO, respectively. Figure 2a shows the

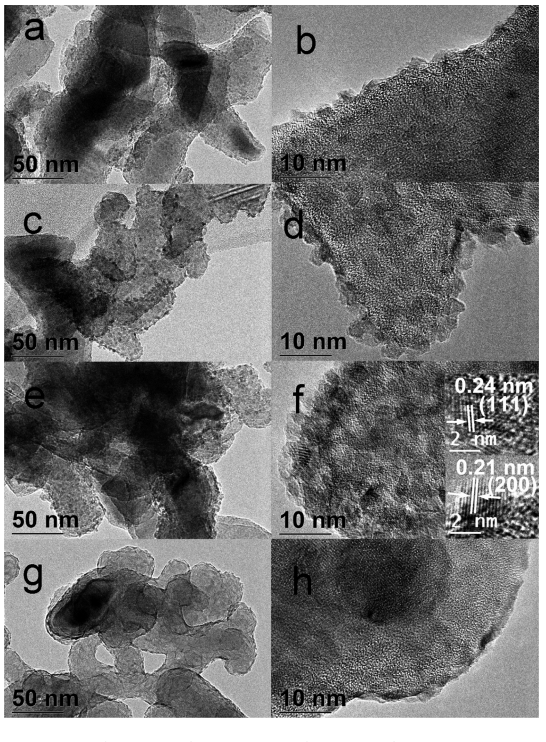

Figure 1. Low (a, c, e, g) and high (b, d, f, h) magnification TEM images of 200-, 400-, 600-, and 800-NiO/SiC. Insets in (f) are high resolution TEM images of 600-NiO/SiC.

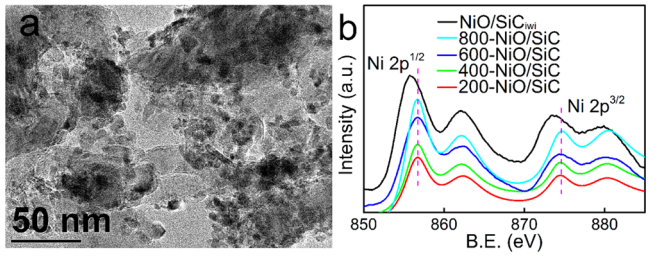

Figure 2. (a) TEM image of NiO/SiC_{iwi} and (b) Ni XPS spectra of ALD-NiO/SiC and NiO/SiC_{iwi}.

DOI: 10.1021/am508508m
ACS Appl. Mater. Interfaces 2015, 7, 4772−4777

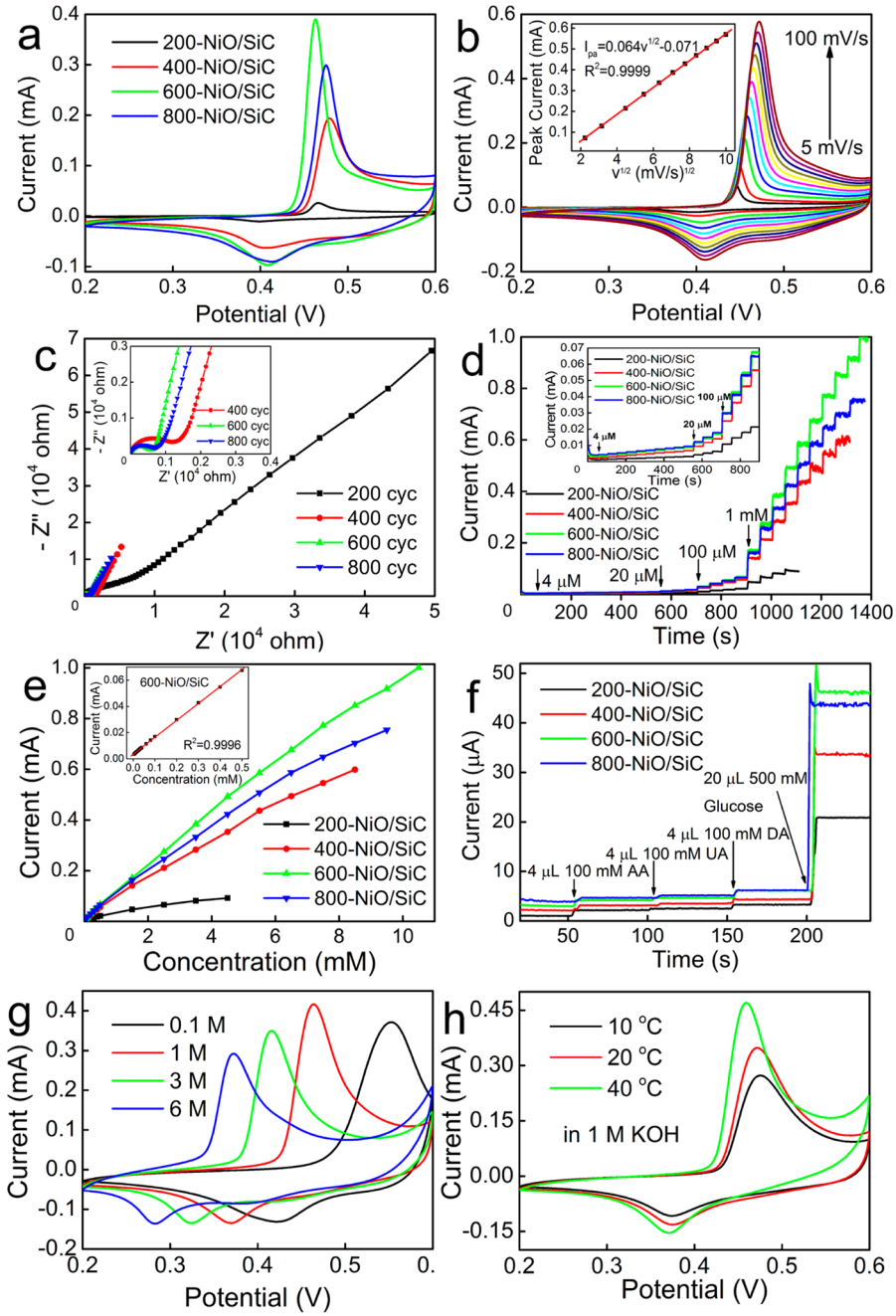

Figure 3. (a) Cyclic voltammograms of NiO/SiC with different ALD cycles in 1 M KOH solution at a scan rate of 50 mV s^{-1}. (b) CV curves of the 600-NiO/SiC modified electrode at various scan rates. The inset shows the relationship between the oxidant peak current and the square root of the scan rate. (c) EIS curves of NiO/SiC samples. The inset shows the EIS curves of 400-, 600-, and 800-NiO/SiC at the high frequency region. (d) Current−time recordings of different NiO/SiC biosensors with successive addition of glucose. (e) Plot of the current versus glucose concentration for the different NiO/SiC biosensors. The inset shows the fitted curve of the current of 600-NiO/SiC varying with glucose concentration from 4 to 500 μM. (f) Amperometric responses of different NiO/SiC biosensors to various interferents and glucose. (g) CV curves of 600-NiO/SiC in different concentrations of KOH solution at 50 mV s^{-1}. (h) CV curves of 600-NiO/SiC at different temperatures in 1 M KOH at 50 mV s^{-1}.

TEM image of NiO/SiC_{iwi}. The size of the NiO nanoparticles is about 5.4 nm on average, which is larger than that of 600-NiO/SiC. Moreover, the dispersity of the NiO nanoparticles is less uniform than that of 600-NiO/SiC.

The Ni contents in 200-, 400-, 600-, and 800-NiO/SiC measured by ICP-AES are approximately 2.88, 6.84, 10.77, and 13.32 wt %, respectively, corresponding to NiO contents of approximately 3.67, 8.71, 13.71, and 16.96 wt %, respectively. XPS was employed to identify the chemical state of the Ni element in 600-NiO/SiC and NiO/SiC_{iwi}, and their Ni 2p profiles are shown in Figure 2b. In the 600-NiO/SiC curve, the peaks located at the binding energies of 856.6 and 874.6 eV are attributed to Ni $2p^{1/2}$ and Ni $2p^{3/2}$, respectively, and the peaks located at the binding energies of 862.6 and 880.8 eV are their satellite peaks, respectively. The binding energy of Ni in 200-, 400-, and 800-NiO/SiC is almost identical to that of 600-NiO/SiC despite the difference in NiO nanoparticle size in the different ALD-NiO/SiC samples. From the NiO/SiC_{iwi} curve, these four peaks are located at 855.9, 862.3, 873.8, and 879.8 eV, respectively. The Ni 2p binding energy of 600-NiO/SiC is

DOI: 10.1021/am508508m
ACS Appl. Mater. Interfaces 2015, 7, 4772−4777

higher than that of the NiO/SiC_{iwi} sample, implying a stronger interaction between the NiO nanoparticles and the SiC substrate in the ALD-synthesized sample, which favors the electron transfer process.[34] The stronger interaction between NiO and SiC in ALD-NiO/SiC may be ascribed to chemical bonding between NiO and SiC that results from the ALD growth mechanism.

Electrochemical Measurements. Figure 3a shows cyclic voltammograms of 200-, 400-, 600-, and 800-NiO/SiC modified electrodes. It can be seen that the onset potentials of these NiO/SiC samples are more negative when the NiO-ALD cycles increase from 200 to 600 cycles. However, further increasing the number of ALD cycles results in an inverse change in the onset potential. The 600-NiO/SiC modified electrode possesses the highest anodic peak current of ~189.42 mA mg^{-1} (with values of 47.99, 147.71, and 116.69 mA mg^{-1} for 200-, 400-, and 800-NiO/SiC, respectively). Figure 3b shows cyclic voltammograms of the modified electrode with the 600-NiO/SiC composite measured at different scan rates (ν). The anodic peak currents grow linearly with the square root of the scan rate (inset of Figure 3b), suggesting a diffusion-controlled electrochemical process, which is an ideal case in quantitative analysis.[32] Figure 3c shows the EIS curves of these samples. A semicircular area at high frequency corresponding to the electron transfer-limited process is observed for each sample. The diameter of the semicircle represents the electron transfer resistance of the electrode material. From Figure 3c, the 600-NiO/SiC electrode exhibits the lowest charge-transfer resistance, which facilitates the electrochemical process. This indicates that NiO nanoparticles in the 600-NiO/SiC sample have more surface active sites than the other samples.

The glucose sensing performance of ALD-NiO/SiC is analyzed by chronoamperometry. Figure 3d shows the amperometric response of different NiO/SiC glucose sensors with successive addition of glucose approximately every 50 s at an applied potential of 0.5 V. Each biosensor exhibits rapid current increase with the addition of 4 μM glucose. With a signal-to-noise (S/N) ratio of 3, the glucose detection limits were calculated to be approximately 0.89, 0.45, 0.32, and 0.93 μM for the 200-, 400-, 600-, and 800-NiO/SiC biosensors, respectively. The calibration curves of these NiO/SiC biosensors are shown in Figure 3e. The 600-NiO/SiC biosensor possesses a linear detection range of up to 7.5 mM, which is higher than that of other samples. In the concentration range from 4 to 500 μM of glucose, these NiO/SiC biosensors exhibit perfect linear amperometric responses to the glucose concentration (inset of Figure 3e shows the linear relationship for 600-NiO/SiC). The glucose sensing sensitivity for 200-, 400-, 600-, and 800-NiO/SiC are approximately 0.580, 1.557, 2.037, and 1.727 mA mM^{-1} cm^{-2}, respectively. From these results, we determined that 600-NiO/SiC exhibits the highest sensitivity and lowest detection limit among these four samples. On the basis of the TEM and EIS analyses, we think that the moderate size of the NiO nanoparticles in 600-NiO/SiC allows for more surface active sites, which contribute to the better performance in glucose sensing. The glucose sensing ability of 600-NiO/SiC is comparable to various Pt, Au, CuO, Co_3O_4, and graphene-based sensors reported in the literature (as listed in Table 1),[12,35−38] demonstrating that the synthesized 600-NiO/SiC is a viable electrode material for glucose sensing.

Anti-interference ability of the NiO/SiC glucose sensors was studied using chronoamperometry experiments with the sequential additions of ascorbic acid (AA), uric acid (UA), dopamine (DA), and glucose in 1 M KOH aqueous solution under 300 rpm magnetic stirring. As shown in Figure 3f, the additions of AA, UA, and DA cause very small increases in the current, whereas the addition of glucose causes a large increase in the current, signifying the high selectivity of the NiO/SiC-based sensor for glucose detection in the presence of coexisting electroactive interference species. The 600-NiO/SiC biosensor exhibits the largest current increase after the addition of glucose, which is consistent with the sensitivity study. A cyclic voltammetry study of the 600-NiO/SiC biosensor was also conducted after 14 days of storage under ambient conditions. The anodic peak current preserves 87% of its initial value, indicating acceptable long-term stability of 600-NiO/SiC.

Table 1. Comparison of the Electrochemical Detection Performance of 600-NiO/SiC with Other Glucose Sensors

electrode	linear range (mM)	detection limit (μM)	sensitivity (mA mM^{-1} cm^{-2})	refs
GOx/PtNP/PAni/Pt	0.01−8	0.7	0.096	12
Cu-N-G	0.004−4.5	1.3	0.681	35
GM-NiO	0.001−0.1	1.6	0.918	36
3D graphene/Co_3O_4	<0.08	<0.025	3.39	37
Au/MNE	0.1−3000	0.5	2.978	38
600-NiO/SiC	0.004−7.5	0.32	2.037	this work

In addition, we investigated the influence of the KOH concentration and temperature on the electrochemical activity of 600-NiO/SiC by cyclic voltammetry. The results are shown in Figure 3g and h. At room temperature, the onset potential in CV curves shifted toward the negative direction when the concentration of KOH solution increased from 0.1 to 6 M (Figure 3g), consistent with previous reports.[39] The peak current is also influenced by the KOH concentration. The highest current response for 600-NiO/SiC is exhibited in 1 M KOH. At high potentials and pH values, some oxidizable compounds may lead to unwanted interference and hindrance of glucose detection.[40] In 1 M KOH, the 600-NiO/SiC electrode works well in the temperature range of 10−40 °C. The current response increases and the onset potential becomes lower as the temperature is increased from 10 to 40 °C. From Figure 3b, it can be seen that the electrochemical reaction at the 600-NiO/SiC electrode is a diffusion-controlled process. Higher temperature promotes the diffusion process, leading to higher current response and lower onset potential.

For comparison, we investigated the glucose sensing ability of bare SiC, commercial NiO, and NiO/SiC_{iwi} by chronoamperometry. Amperometric responses of these biosensors to the stepwise addition of glucose are shown in Figure 4. The bare SiC-modified electrode exhibits no response toward the addition of glucose. The commercial NiO-modified electrode exhibits an apparent current increase with the addition of glucose, but the current increment declines quickly with the successive addition of glucose, implying an inferior detection range. The linear detection range of commercial NiO may be damaged from the dissolution or aggregation of NiO nanoparticles.[41] The NiO/SiC_{iwi}-modified electrode exhibits a small current increase (~1/6 of 600-NiO/SiC) with the addition of glucose. The glucose sensing performance of 600-NiO/SiC being better than that of NiO/SiC_{iwi} should be attributed to the good dispersity of NiO nanoparticles and the strong interaction between the NiO nanoparticles and SiC

DOI: 10.1021/am508508m
ACS Appl. Mater. Interfaces 2015, 7, 4772−4777

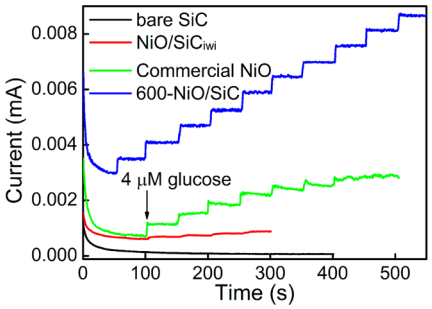

Figure 4. Comparison of the glucose sensing ability of 600-NiO/SiC to other materials.

substrate, as revealed by TEM and XPS characterization. The strong interaction between NiO and SiC in 600-NiO/SiC also reduces the dissolution and aggregation of NiO nanoparticles, thus leading to a wider glucose detection range.

CONCLUSION

In this study, NiO nanoparticles were grown on SiC particles by ALD with high dispersity and uniform particle size. The 600-NiO/SiC nanocomposite exhibits the best glucose sensing capacity among the materials we investigated. With a comparison to NiO/SiC$_{iwi}$ made through the impregnation method, it is clear that ALD is advantageous for making an electrochemical active substance for biosensing applications due to its precise size control of the deposited materials and the strong interaction between the deposited materials and the substrate. In addition, SiC is a superb substrate in electrochemical biosensing due to its biocompatibility, low background current, and broad electrochemical potential window. It is highly expected that the combination of NiO ALD and SiC substrate will find potential applications in bioprocess monitoring, medical diagnosis, the food industry, and so forth.

AUTHOR INFORMATION

Corresponding Author

*E-mail: qinyong@sxicc.ac.cn. Fax: +86 351 4040081. Tel: +86 351 4040081.

Notes

The authors declare no competing financial interest.

ACKNOWLEDGMENTS

This work was financially supported by National Natural Science Foundation of China (21173248, 21376256, and 21203229), the Hundred Talent Program of the Chinese Academy of Sciences, the Hundred Talent Program of Shanxi Province, and an in-house project of the State Key Laboratory of Coal Conversion of China (Y3BWLE1931).

REFERENCES

(1) Tominaga, M.; Shimazoe, T.; Nagashima, M.; Taniguchi, I. Electrocatalytic Oxidation of Glucose at Gold Nanoparticle-Modified Carbon Electrodes in Alkaline and Neutral Solutions. *Electrochem. Commun.* **2005**, *7*, 189−193.

(2) Nan, C. F.; Zhang, Y.; Zhang, G. M.; Dong, C.; Shuang, S. M.; Choi, M. M. F. Activation of Nylon Net and Its Application to a Biosensor for Determination of Glucose in Human Serum. *Enzyme Microb. Technol.* **2009**, *44*, 249−253.

(3) Curey, T. E.; Salazar, M. A.; Oliveira, P.; Javier, J.; Dennis, P. J.; Rao, P.; Shear, J. B. Enzyme-Based Sensor Arrays for Rapid Characterization of Complex Disaccharide Solutions. *Anal. Biochem.* **2002**, *303*, 42−48.

(4) Ci, S. Q.; Huang, T. Z.; Wen, Z. H.; Cui, S. M.; Mao, S.; Steeber, D. A.; Chen, J. H. Nickel Oxide Hollow Microsphere for Non-Enzyme Glucose Detection. *Biosens. Bioelectron.* **2014**, *54*, 251−257.

(5) Arnold, M. A.; Small, G. W. Noninvasive Glucose Sensing. *Anal. Chem.* **2005**, *77*, 5429−5439.

(6) Wang, J.; Thomas, D. F.; Chen, A. Nonenzymatic Electrochemical Glucose Sensor Based on Nanoporous PtPb Networks. *Anal. Chem.* **2008**, *80*, 997−1004.

(7) Wang, J. Electrochemical Glucose Biosensors. *Chem. Rev.* **2008**, *108*, 814−825.

(8) Clark, L. C.; Lyons, C. Electrode Systems for Continuous Monitoring in Cardiovascular Surgery. *Ann. N.Y. Acad. Sci.* **1962**, *102*, 29−45.

(9) Kong, T.; Chen, Y.; Ye, Y. P.; Zhang, K.; Wang, Z. X.; Wang, X. P. An Amperometric Glucose Biosensor Based on the Immobilization of Glucose Oxidase on the Zno Nanotubes. *Sens. Actuators, B* **2009**, *138*, 344−350.

(10) Park, S.; Boo, H.; Chung, T. D. Electrochemical Non-Enzymatic Glucose Sensors. *Anal. Chim. Acta* **2006**, *556*, 46−57.

(11) Bai, L. J.; Yuan, R.; Chai, Y. Q.; Zhuo, Y.; Yuan, Y. L.; Wang, Y. Simultaneous Electrochemical Detection of Multiple Analytes Based on Dual Signal Amplification of Single-Walled Carbon Nanotubes and Multi-Labeled Graphene Sheets. *Biomaterials* **2012**, *33*, 1090−1096.

(12) Zhai, D. Y.; Liu, B. R.; Shi, Y.; Pan, L. J.; Wang, Y. Q.; Li, W. B.; Zhang, R.; Yu, G. H. Highly Sensitive Glucose Sensor Based on Pt Nanoparticle/Polyaniline Hydrogel Heterostructures. *ACS Nano* **2013**, *7*, 3540−3546.

(13) Yang, Z.; Zong, X. L.; Ye, Z. Z.; Zhao, B. H.; Wang, Q. L.; Wang, P. The Application of Complex Multiple Forklike Zno Nanostructures to Rapid and Ultrahigh Sensitive Hydrogen Peroxide Biosensors. *Biomaterials* **2010**, *31*, 7534−7541.

(14) El-Refaei, S. M.; Saleh, M. M.; Awad, M. I. Enhanced Glucose Electrooxidation at a Binary Catalyst of Manganese and Nickel Oxides Modified Glassy Carbon Electrode. *J. Power Sources* **2013**, *223*, 125−128.

(15) Cao, F.; Guo, S.; Ma, H. Y.; Shan, D. C.; Yang, S. X.; Gong, J. A. Nickel Oxide Microfibers Immobilized onto Electrode by Electrospinning and Calcination for Nonenzymatic Glucose Sensor and Effect of Calcination Temperature on the Performance. *Biosens. Bioelectron.* **2011**, *26*, 2756−2760.

(16) Park, S.-Y.; Seo, H. O.; Kim, K.-D.; Shim, W. H.; Heo, J.; Cho, S.; Kim, Y. D.; Lee, K. H.; Lim, D. C. Organic Solar Cells Fabricated by One-Step Deposition of a Bulk Heterojunction Mixture and TiO_2/NiO Hole-Collecting Agents. *J. Phys. Chem. C* **2012**, *116*, 15348−15352.

(17) Wang, G. M.; Lu, X. H.; Zhai, T.; Ling, Y. C.; Wang, H. Y.; Tong, Y. X.; Li, Y. Free-Standing Nickel Oxide Nanoflake Arrays: Synthesis and Application for Highly Sensitive Non-Enzymatic Glucose Sensors. *Nanoscale* **2012**, *4*, 3123−3127.

(18) Zhang, W. D.; Chen, J.; Jiang, L. C.; Yu, Y. X.; Zhang, J. Q. A Highly Sensitive Nonenzymatic Glucose Sensor Based on NiO-Modified Multi-Walled Carbon Nanotubes. *Microchim. Acta* **2010**, *168*, 259−265.

(19) Gangopadhyay, R.; De, A. Conducting Polymer Nanocomposites: A Brief Overview. *Chem. Mater.* **2000**, *12*, 608−622.

(20) Mu, Y.; Jia, D.; He, Y.; Miao, Y.; Wu, H.-L. Nano Nickel Oxide Modified Non-Enzymatic Glucose Sensors with Enhanced Sensitivity through an Electrochemical Process Strategy at High Potential. *Biosens. Bioelectron.* **2011**, *26*, 2948−2952.

(21) Liu, S.; Yu, B.; Zhang, T. A Novel Non-Enzymatic Glucose Sensor Based on Nio Hollow Spheres. *Electrochim. Acta* **2013**, *102*, 104−107.

(22) Li, X.; Hu, A. Z.; Jiang, J.; Ding, R. M.; Liu, J. P.; Huang, X. T. Preparation of Nickel Oxide and Carbon Nanosheet Array and Its Application in Glucose Sensing. *J. Solid State Chem.* **2011**, *184*, 2738−2743.

DOI: 10.1021/am508508m
ACS Appl. Mater. Interfaces 2015, 7, 4772−4777

(23) Salimi, A.; Roushani, M. Non-Enzymatic Glucose Detection Free of Ascorbic Acid Interference Using Nickel Powder and Nafion Sol-Gel Dispersed Renewable Carbon Ceramic Electrode. *Electrochem. Commun.* **2005**, *7*, 879−887.
(24) Salimi, A.; Roushani, M.; Soltanian, S.; Hallaj, R. Picomolar Detection of Insulin at Renewable Nickel Powder-Doped Carbon Composite Electrode. *Anal. Chem.* **2007**, *79*, 7431−7438.
(25) Lu, J. L.; Elam, J. W.; Stair, P. C. Synthesis and Stabilization of Supported Metal Catalysts by Atomic Layer Deposition. *Acc. Chem. Res.* **2013**, *46*, 1806−1815.
(26) Choi, T.; Kim, S. H.; Lee, C. W.; Kim, H.; Choi, S.-K.; Kim, S.-H.; Kim, E.; Park, J.; Kim, H. Synthesis of Carbon Nanotube-Nickel Nanocomposites Using Atomic Layer Deposition for High-Performance Non-Enzymatic Glucose Sensing. *Biosens. Bioelectron.* **2015**, *63*, 325−330.
(27) Tong, X. L.; Qin, Y.; Guo, X. Y.; Moutanabbir, O.; Ao, X. Y.; Pippel, E.; Zhang, L. B.; Knez, M. Enhanced Catalytic Activity for Methanol Electro-Oxidation of Uniformly Dispersed Nickel Oxide Nanoparticles-Carbon Nanotube Hybrid Materials. *Small* **2012**, *8*, 3390−3395.
(28) Zhao, H. S.; Shi, L. M.; Li, Z. Q.; Tang, C. H. Silicon Carbide Nanowires Synthesized with Phenolic Resin and Silicon Powders. *Phys. E (Amsterdam, Neth.).* **2009**, *41*, 753−756.
(29) Casady, J. B.; Johnson, R. W. Status of Silicon Carbide (SiC) as a Wide-Bandgap Semiconductor for High-Temperature Applications: A Review. *Solid-State Electron.* **1996**, *39*, 1409−1422.
(30) Gonzalez, P.; Serra, J.; Liste, S.; Chiussi, S.; Leon, B.; Perez-Amor, M.; Martinez-Fernandez, J.; de Arellano-Lopez, A. R.; Varela-Feria, F. M. New Biomorphic SiC Ceramics Coated with Bioactive Glass for Biomedical Applications. *Biomaterials* **2003**, *24*, 4827−4832.
(31) Yang, N.; Zhuang, H.; Hoffmann, R.; Smirnov, W.; Hees, J.; Jiang, X.; Nebel, C. E. Nanocrystalline 3C-SiC Electrode for Biosensing Applications. *Anal. Chem.* **2011**, *83*, 5827−5830.
(32) Salimi, A.; Mohamadi, L.; Hallaj, R.; Soltanian, S. Electro-oxidation of Insulin at Silicon Carbide Nanoparticles Modified Glassy Carbon Electrode. *Electrochem. Commun.* **2009**, *11*, 1116−1119.
(33) Guo, X. N.; Brault, P.; Zhi, G. J.; Caillard, A.; Jin, G. Q.; Coutanceau, C.; Baranton, S.; Guo, X. Y. Synergistic Combination of Plasma Sputtered Pd-Au Bimetallic Nanoparticles for Catalytic Methane Combustion. *J. Phys. Chem. C* **2011**, *115*, 11240−11246.
(34) Wang, M. M.; Chen, J. J.; Liao, X.; Liu, Z. X.; Zhang, J. D.; Gao, L.; Li, Y. Highly Efficient Photocatalytic Hydrogen Production of Platinum Nanoparticle-Decorated SiC Nanowires under Simulated Sunlight Irradiation. *Int. J. Hydrogen Energy* **2014**, *39*, 14581−14587.
(35) Jiang, D.; Liu, Q.; Wang, K.; Qian, J.; Dong, X. Y.; Yang, Z. T.; Du, X. J.; Qiu, B. J. Enhanced Non-Enzymatic Glucose Sensing Based on Copper Nanoparticles Decorated Nitrogen-Doped Graphene. *Biosens. Bioelectron.* **2014**, *54*, 273−278.
(36) Liu, J. J.; Lv, W.; Wei, W.; Zhang, C.; Li, Z. J.; Li, B. H.; Kang, F. Y.; Yang, Q. H. A Three-Dimensional Graphene Skeleton as a Fast Electron and Ion Transport Network for Electrochemical Applications. *J. Mater. Chem. A* **2014**, *2*, 3031−3037.
(37) Dong, X. C.; Xu, H.; Wang, X. W.; Huang, Y. X.; Chan-Park, M. B.; Zhang, H.; Wang, L. H.; Huang, W.; Chen, P. 3D Graphene-Cobalt Oxide Electrode for High-Performance Supercapacitor and Enzymeless Glucose Detection. *ACS Nano* **2012**, *6*, 3206−3213.
(38) Ling, T. R.; Li, C. S.; Jow, J. J.; Lee, J. F. Mesoporous Nickel Electrodes Plated with Gold for the Detection of Glucose. *Electrochim. Acta* **2011**, *56*, 1043−1050.
(39) Li, K.; Fan, G. L.; Yang, L.; Li, F. Novel Ultrasensitive Non-Enzymatic Glucose Sensors Based on Controlled Flower-Like Cuo Hierarchical Films. *Sens. Actuators, B* **2014**, *199*, 175−182.
(40) Yang, J.; Zhang, W. D.; Gunasekaran, S. A Low-Potential, H_2O_2-Assisted Electrodeposition of Cobalt Oxide/Hydroxide Nanostructures onto Vertically-Aligned Multi-Walled Carbon Nanotube Arrays for Glucose Sensing. *Electrochim. Acta* **2011**, *56*, 5538−5544.
(41) Guo, S. J.; Zhang, S.; Sun, X. L.; Sun, S. H. Synthesis of Ultrathin FePtPd Nanowires and Their Use as Catalysts for Methanol Oxidation Reaction. *J. Am. Chem. Soc.* **2011**, *133*, 15354−15357.

DOI: 10.1021/am508508m
ACS Appl. Mater. Interfaces 2015, 7, 4772−4777